JOURNAL OF MATERIALS SCIENCE 26 (1991) 1368–1374

Nucleation, growth and morphology of poly(hydroxybutyrate) and its copolymers

S. J. ORGAN, P. J. BARHAM
H.H. Wills Physics Laboratory, University of Bristol, Tyndall Avenue, Bristol BS8 1TL, UK

Measurements of the melting temperatures, growth rates and nucleation rates of melt-crystallized polyhydroxybutyrate (PHB) and two poly(hydroxybutyrate-co-hydroxyvalerate) (PHB/HV) copolymers are reported for crystallization over a wide range of temperature. Examples are shown of the spherulitic morphologies obtained. From the variation in melting point with crystallization temperature values for the equilibrium melting points of PHB and PHB/HV are obtained. Growth and nucleation rate measurements are analysed using secondary nucleation theory to obtain approximations to surface energies within the crystals. PHB and PHB/7% HV are described well by secondary nucleation theory. PHB/23% HV exhibits more complex crystallization and melting behaviour, which suggests temperature-dependent exclusion of HV units from the crystals.

1. Introduction

Environmental issues are becoming increasingly important as the general public becomes aware of the problems. It is therefore very appropriate that polymer materials which can readily replace many synthetics and which can degrade fully in the environment without forming any toxic products should now be beginning to become available. One such polymer is poly(3-hydroxybutyrate) (PHB) which is formed by many bacteria as an energy storage product [1–7]. This material has the particular advantage that it is a thermoplastic and can therefore, in principle, be processed using existing equipment. However, there are also several drawbacks to the use of PHB, chiefly its tendency to be rather brittle. One solution to this problem is to develop co-polymers of hydroxybutyrate and hydroxyvalerate by feeding bacteria with propionic acid [8]. ICI biological products division is now producing a range of PHB homopolymers and PHB/HV copolymers under the trade name "Biopol". We have already carried out extensive studies of the morphology, crystallization and mechanical behaviour of the homopolymer [9–11] which we are now expanding to include the copolymers. A technique for revealing the lamellar morphology (as revealed by electron microscopy) of these copolymers has been published previously [12]. In this paper we extend this work further and report data for melting points, growth and nucleation rates of copolymers, which will be useful for anyone wishing to process these materials. In addition we shall, for completeness, show the morphologies of the various polymers used and we shall discuss the implications of our findings for the crystallization mechanisms in PHB/HV copolymers.

2. Experimental procedure

Melting points, T_m, growth rates, G, and nucleation rates, I, were measured on the following three samples: PHB homopolymer with $M_W = 410\,000$ $M_W/M_n = 2.4$; PHB/HV copolymer containing 7% HV (PHB/7% HV) with $M_W = 470\,000$, $M_W/M_n = 3.7$; PHB/HV copolymer containing 23% HV (PHB/23% HV) with $M_W = 450\,000$, $M_W/M_n = 3.0$.

The molecular weights were measured by gel permeation chromatography calibrated using polystyrene standards and have been corrected to true molecular weights in each case by using constants obtained for PHB in the Mark–Houwink relationship. Melting points were measured by differential scanning calorimetry (DSC) using a Perkin–Elmer DSC-7. For each measurement a few milligrams of polymer in a sealed pan were melted for 2 min in the DSC. The melting points used were 200, 190 and 180 °C for PHB, PHB/7%HV and PHB/23% HV, respectively, chosen to avoid any seeding effects. Each sample was then cooled to a crystallization temperature (T_c) in the range 40 to 125 °C and left until crystallization was complete, as judged from the associated exotherm. Crystallization times were thus the minimum required at a particular temperature for complete crystallization and varied between samples from a few minutes to several hours. This method was chosen so as to minimize annealing effects. Samples were subsequently heated at 20 °C min^{-1} and the position of any melting endotherm measured. Results were corrected to allow for heating rate and calibrated using indium.

Growth and nucleation rates were measured by optical microscopy. Thin samples were prepared between microscope cover slips. The samples were melted as described previously and cooled at 99 °C min^{-1} to the required crystallization temperature in a nitrogen-cooled Linkam THMS600 microscope hot stage, coupled to a TMS90 temperature controller. A Zeiss Ultraphot polarizing microscope was used to view the samples. Crystallization was recorded using a U-matic

0022-2461/91 $03.00 + .12

video system which included timing and measuring devices. This allowed even the fastest rates to be measured easily and accurately from the video screen. Nucleation rates were measured by counting the number of nuclei within a known volume of sample after successive time intervals until the point when approximately 20% of the sample had crystallized. Results varied considerably and many measurements were made at each temperature. For growth rate measurements a new sample was used each time to avoid any effects due to degradation; for nucleation rate measurement samples were used a maximum of three times.

3. Results

3.1. Morphology

Fig. 1 shows a series of optical micrographs showing the spherulitic texture of the three materials used crystallized at 60 and 100 °C. In all cases large spherulites were observed. In most cases banding is visible, although the regularity of the banding, as well as the band spacing, varies considerably with crystallization conditions. Spherulites from PHB and PHB/7% HV are more birefringent than PHB/23% HV and generally have a more regular texture. Differences in nucleation and growth rates are obvious from the number and age of the spherulites in the various samples: these differences are quantified below. Similar morphologies can be observed on a lamellar scale from replicas of samples which have been etched using methylamine [12]. Fig. 2 shows examples of the typical sheaf-like morphology found at the centre of spherulites (Fig. 2a), the regular twisting lamellae seen further out along the radius of a large spherulite (Fig. 2b) and a more irregular lamellar arrangement often obtained from copolymer samples crystallized at temperatures where the growth rate is relatively high (Fig. 2c). The regularly spaced holes in Fig. 2b are likely to arise from regions where the etchant has penetrated more deeply and probably indicate HV-rich areas.

3.2. Melting points

Samples of PHB and PHB/7% HV had reasonably sharp melting points (T_m) which increased with T_c. Even using a fast heating rate of 20 °C min^{-1} most samples underwent some thickening during the DSC scan, resulting in a double melting peak as shown in Fig. 3. For the lower crystallization temperatures, the degree of thickening was such that the original (lower) melting peak was barely discernible, while for the higher crystallization temperatures little or no thickening occurred. The variation in T_m with T_c is shown in Figs 4 and 5 for samples of PHB and PHB/7% HV, respectively. The melting points shown are the peak position, measured from the endotherm corresponding to the original, non-annealed crystals. No accurate values could be obtained from samples grown at the lower crystallization temperatures due to annealing during heating. Approximate values have been obtained for the equilibrium melting temperature, T_m^0, by extrapolating the T_m against T_c curve to the point where $T_m = T_c$ [13]. The values obtained are $T_m^0 = 188.0 \pm 2.0$ °C for PHB and $T_m^0 = 173.0 \pm 2.5$ °C for PHB/7% HV. The figure obtained for PHB is lower than that published previously [9] (195 ± 5 °C), possibly due to the shorter crystallization times used in this study. An alternative value of T_m^0 might be obtained by taking the maximum value of T_m in each case, because this corresponds to the most perfect crystal within that sample. However, the maximum measured melting point is highly affected by any annealing and the value obtained is therefore somewhat arbitrary and usually rather low.

The melting behaviour of the copolymer with higher HV content, PHB/23% HV was far more complex. Fig. 6 shows examples of the DSC traces obtained after crystallization at 50 and 80 °C. Five separate peaks can be identified (labelled a to e in Fig. 6) and these were present in all traces, although their relative heights varied considerably depending on crystallization conditions. The position of each peak varied systematically with crystallization temperature as shown in Fig. 7. A detailed analysis of the content of the different peaks will not be attempted here, but from studying the effect of crystallization temperature, crystallization time (t_c), DSC heating rate and the time a sample was left at room temperature before melting, on the melting behaviour, a few general statements may be made as to their possible origin.

(i) Peak A has $T_m \simeq T_c$. The relative area of this peak increases with T_c and with the time a sample is left at room temperature before melting. It probably arises from material which cannot easily crystallize at T_c and which crystallizes subsequently when the sample is cooled.

(ii) Peaks B and C are associated with crystallization at T_c. Peak C is always the largest and sharpest peak and represents the majority of crystals which grow at T_c.

(iii) Peak D increases at the expense of peak C if the DSC heating rate is lowered, suggesting that it arises from annealing of crystals during heating. The relative area of peak D decreases as T_c is raised, as would be expected.

(iv) Peak E is small and has relatively constant position and area. It may correspond to a PHB impurity or a PHB-rich phase with the sample.

The presence of multiple melting peaks and their considerable variation with crystallization conditions and subsequent thermal treatment has important implications for the crystallization mechanism in PHB/HV copolymers, which will be considered further in the discussion section. If we take peak C to represent the "true" melting point of 23% HV copolymer and extrapolate the T_m against T_c curve to $T_m = T_c$ as before, we obtain a value of $T_m^0 = 186.2 \pm 3.0$ °C (see Fig. 7). This is much higher than would be expected for such a copolymer and is very close to the value obtained for PHB. It is likely that this result reflects a systematic increase with T_c in the percentage of PHB incorporated into the crystalline portion of the sample, implying the possibility of substantial exclusion of HV from the crystal lattice.

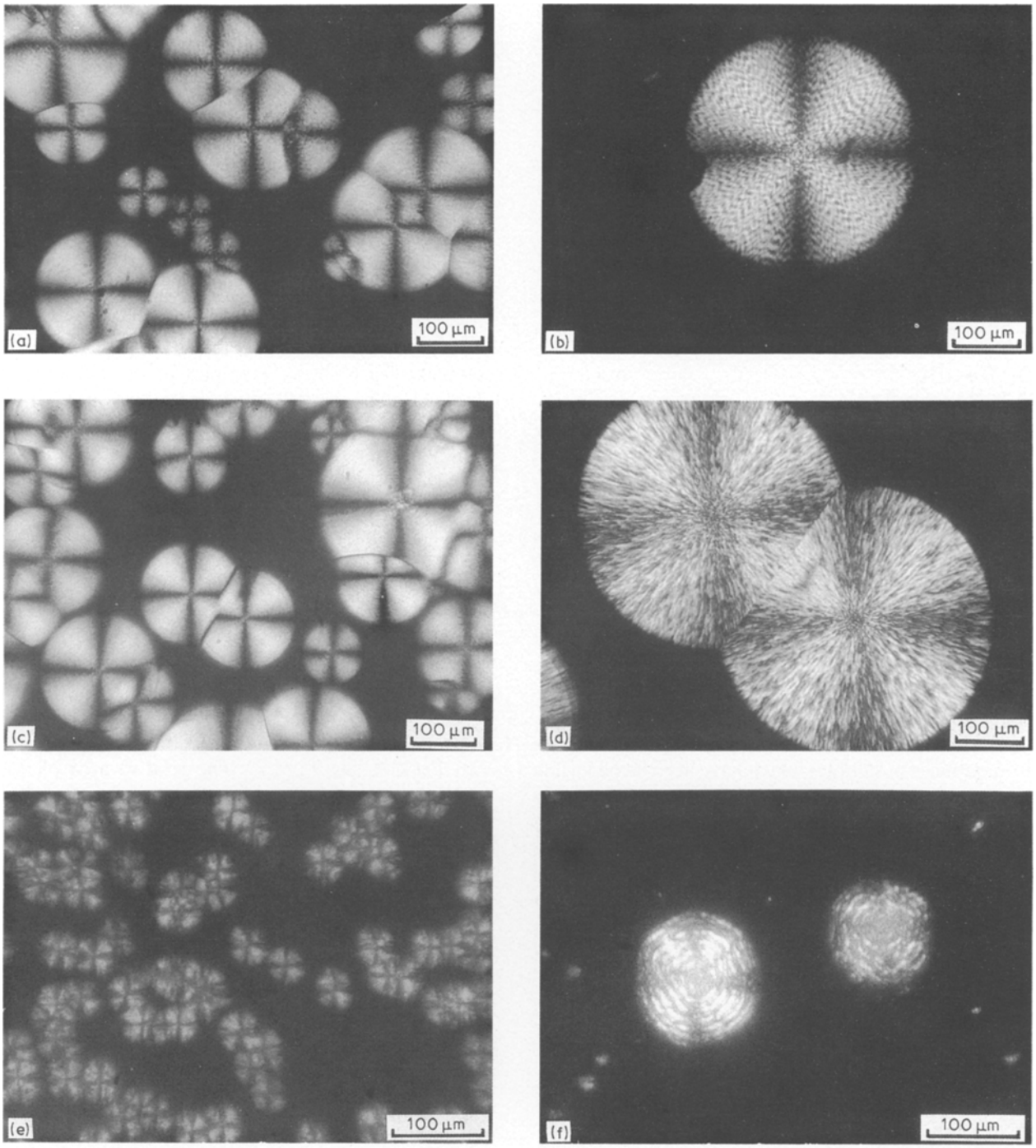

Figure 1 Spherulitic morphologies viewed under crossed polars. (a) PHB, $T_c = 60\,°C$, $t_c = 1$ min. (b) PHB, $T_c = 100\,°C$, $t_c = 3$ min. (c) PHB/7% HV, $T_c = 60\,°C$, $t_c = 2.5$ min. (d) PHB/7% HV, $T_c = 100\,°C$, $t_c = 5.5$ min. (e) PHB/23% HV, $T_c = 60\,°C$, $t_c = 1\,h\ 15$ min. (f) PHB/23% HV, $T_c = 100\,°C$, $t_c = 45$ min.

3.3. Growth and nucleation rates

All three samples grew as spherulites, as shown in Fig. 1, although those of PHB/23% HV were only weakly birefringent and were difficult to see. Radial growth rates were found to be linear in all cases. The variations in growth rate with crystallization temperature are shown in Fig. 8. It can be seen that the low rates in PHB are considerably reduced by the addition of HV. In addition, the maximum of the growth rate curve shifts to lower temperatures as the HV content is increased. The corresponding nucleation rates, I, are shown in Fig. 9; again the addition of HV units has a pronounced effect, both on the magnitude of the rates and on the temperature at which the maximum occurs. Nucleation rates were more or less constant during the early stages of growth, although the associated errors are large – some representative error bars are included in Fig. 9.

3.4. Analysis of growth and nucleation rate data

The kinetic theory of polymer crystallization may be used to analyse the growth and nucleation rate data and obtain values for surface energies within the crystals. Hoffman [14] gives the linear growth rate of

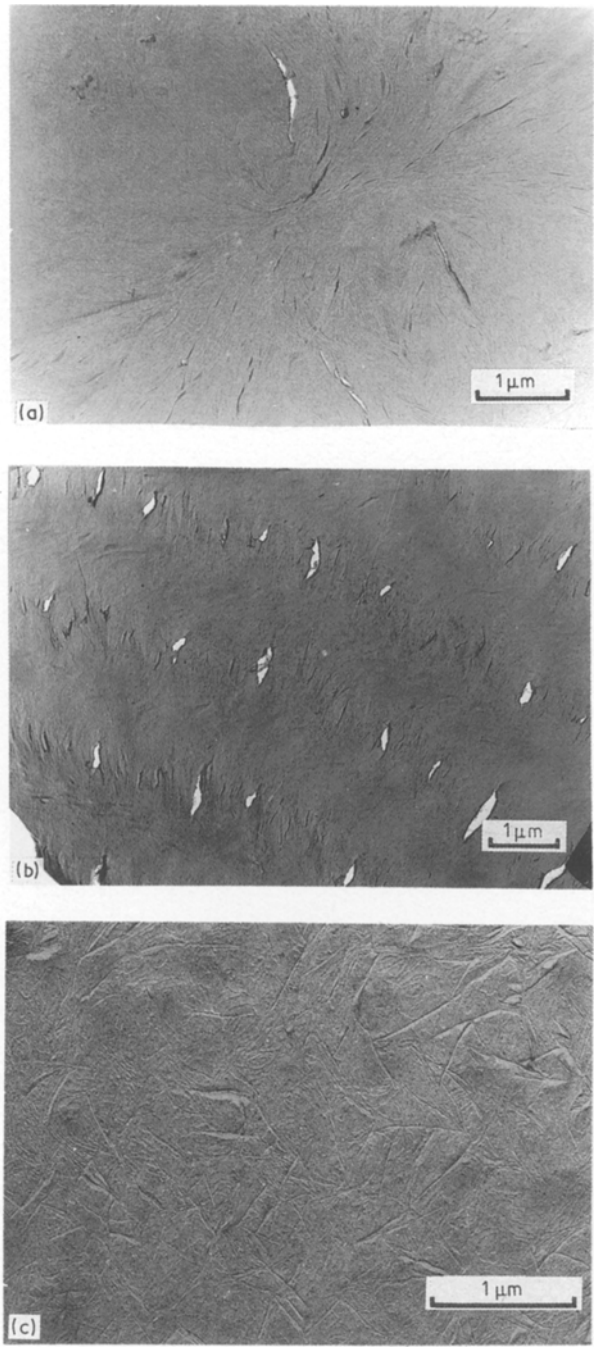

Figure 2 Electron micrographs showing examples of lamellar morphologies revealed by etching with methylamine. (a) Sheaf-like morphology typically found at the centre of a spherulite. (b) Lamellar twisting along the radius of a spherulite in a high HV copolymer showing the origin of the banding. Radial direction arrowed. (c) Irregular structure typically obtained from copolymers crystallized at temperatures where the growth rate is relatively high.

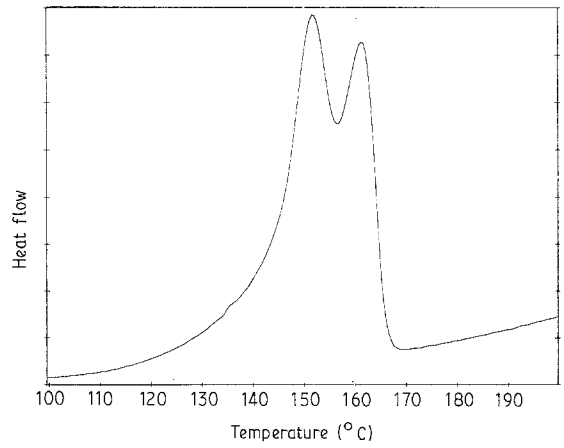

Figure 3 Differential scanning calorimetry trace showing double melting peak obtained from PHB/7% HV crystallized at 70 °C.

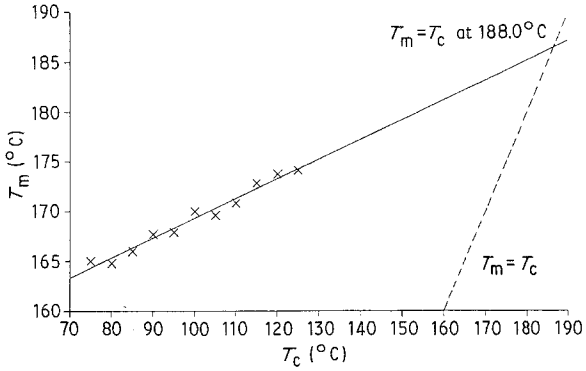

Figure 4 Increase in melting point, T_m, with crystallization temperature, T_c, for PHB homopolymer.

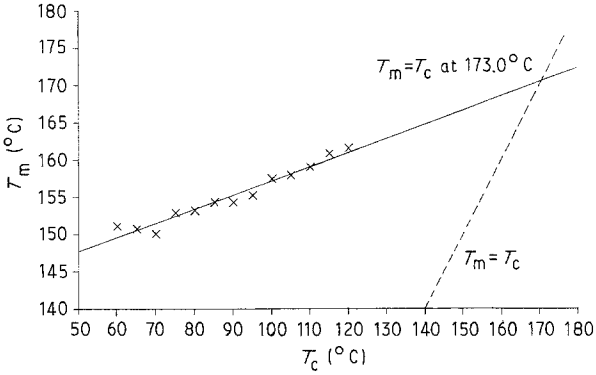

Figure 5 Increase in melting point, T_m, with crystallization temperature, T_c, for PHV/7% HV copolymer.

spherulites as

$$G = G_0 \exp[-U^*/R(T_c - T_\infty)] \exp(-Kb\sigma\sigma_e T_m^0/\Delta H \Delta T k T_c) \quad (1)$$

where G_0 is a constant, U^* is an activation energy for transport of molecules to the growth front, R is the gas constant, T_∞ is the temperature below which molecules become immobile, ΔH is the heat of fusion, ΔT is the supercooling ($T_m^0 - T_c$), k is Boltzmann's constant and σ and σ_e are the side surface and end surface free energies, respectively. K may have the value 2 or 4, depending on the relative rates of secondary nucleation and spreading along the growth front of the crystal. Hoffman predicts three regimes: in regime I the rate of spreading is much greater than the rate of nucleation, so that once a nucleus has formed it will spread rapidly across a "substrate length" on the growth front; in regime II several nuclei may form and spread across the substrate together; in regime III the separation of nuclei is comparable with the molecular width so that no spreading occurs.

Previous work on PHB measured the heat of fusion to be 1.85×10^8 J m^{-3} and found best fit values of

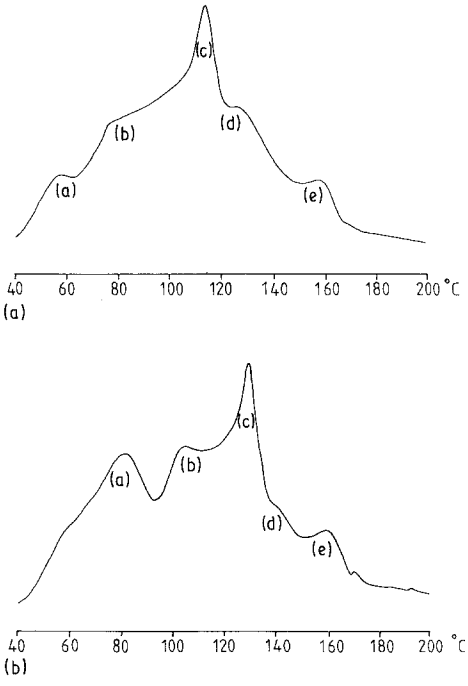

Figure 6 Examples of the DSC thermograms obtained on melting PHB/23% HV copolymer. (a) $T_c = 50\,°C$, (b) $T_c = 80\,°C$.

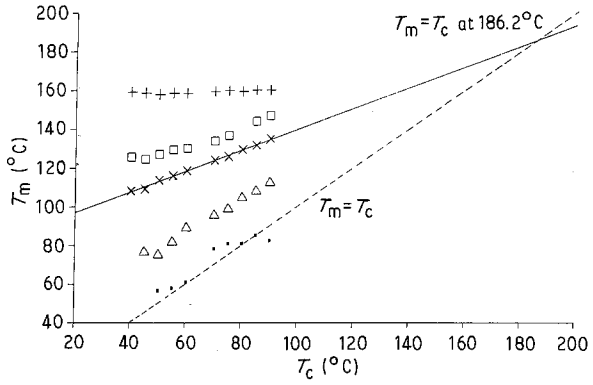

Figure 7 Variation in melting point, T_m, with crystallization temperature, T_c, for PHB/23% HV copolymer. The peaks a to e are as indicated on Fig. 6: (■) a, (△) b, (×) c, (□) d, (+) e.

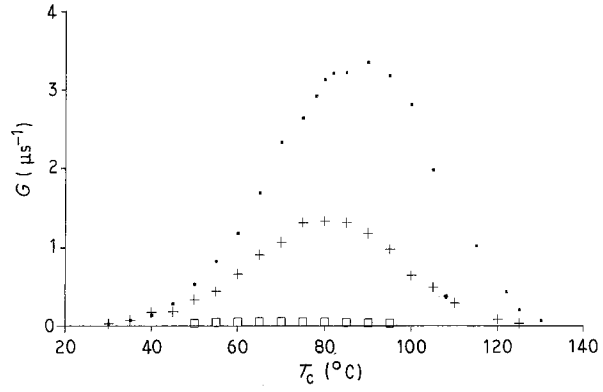

Figure 8 Variation of radial spherulite growth rate, G, with crystallization temperature, T_c, for (■) PHB and two copolymers: (+) 7% HV; (□) 23% HV.

$U^* = 10.25\,\text{kJ mol}^{-1}$ and $T_\infty = -48\,°C$. Crystallization was shown to be in regime III for $T_c < 130\,°C$, with $K = 4$. Using the above values for ΔH, U^*, T_∞ and K, $T_m^0 = 188.0\,°C$ from this work, and taking

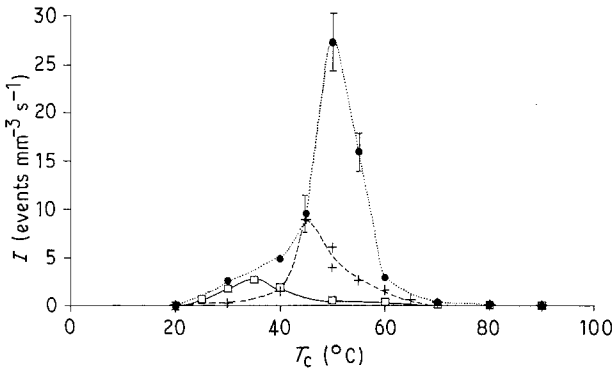

Figure 9 Variation of nucleation rate, I, with crystallization temperature, T_c, for (●) PHB and two copolymers: (+) 7% HV; (□) 23% HV.

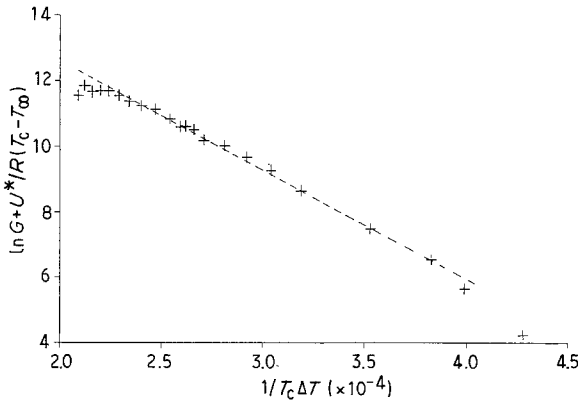

Figure 10 Analysis of growth rate data for PHB using the kinetic theory of crystallization.

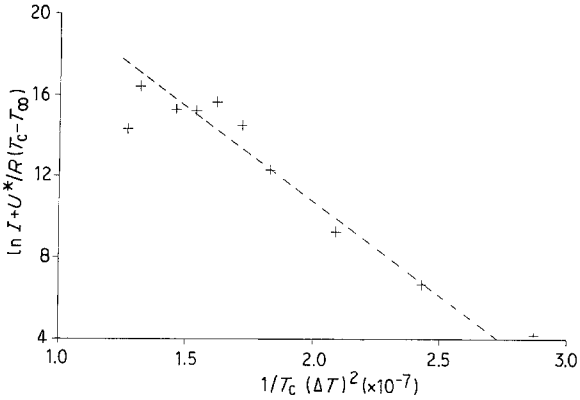

Figure 11 Analysis of nucleation rate data for PHB.

$k = 1.38 \times 10^{-23}\,\text{J K}^{-1}$, $b = 5.8 \times 10^{-10}\,\text{m}$, we may plot $\ln G + U^*/R(T_c - T_\infty)$ against $1/T_c\Delta T$ and obtain a value for $\sigma\sigma_e$. Such a plot is shown in Fig. 10 for PHB; the data give a reasonable straight line and yield a value of $\sigma\sigma_e = 7.73 \times 10^{-4}\,(\text{J m}^{-2})^2$.

Homogeneous nucleation theory predicts [15]

$$I = I_0 \exp[-U^*/R(T_c - T_\infty)] \exp [-32\sigma^2\sigma_e(T_m^0)^2/(\Delta H)^2(\Delta T)^2 kT] \quad (2)$$

where I_0 is a constant and this relationship is plotted in Fig. 11 for PHB using the same values as above. From the gradient of the graph we obtain $\sigma^2\sigma_e = 6.363 \times 10^{-6}\,(\text{J m}^{-2})^3$, which taken together with

the result from the growth rate analysis yields $\sigma = 8.2 \times 10^{-3}\,J\,m^{-2}$ and $\sigma_e = 93.9 \times 10^{-3}\,J\,m^{-2}$. These values are well within the expected range.

The same analysis may be used for PHB/7% HV. Fig. 12 shows a plot of $\ln G + U^*/R(T_c - T_\infty)$ against $1/T_c\Delta T$ assuming the same values for U^* and T_∞ and taking $T_m^0 = 173.0\,°C$. The data give a straight line and from the gradient (assuming b is that of the PHB lattice) we obtain $\sigma\sigma_e/\Delta H = 3.71 \times 10^{-9}\,J\,m^{-1}$. The heat of fusion of this copolymer has not been measured directly, but from other work [16] a reasonable value is $\Delta H = 1.65 \times 10^8\,J\,m^{-3}$. Thus we obtain $\sigma\sigma_e = 6.12 \times 10^{-4}\,(J\,m^{-2})^2$. The nucleation rate data are plotted in Fig. 13. At the lower crystallization temperatures the analysis works well, but at higher temperatures there is a sharp deviation. Taking the gradient from the lower temperature points only, we obtain $\sigma^2\sigma_e = 3.115 \times 10^{-6}\,(J\,m^{-2})^3$, and thus $\sigma = 5.1 \times 10^{-3}$ and $\sigma_e = 120.2 \times 10^{-3}\,J\,m^{-2}$. The nucleation rates measured at the higher crystallization temperatures are much faster than the values which would be expected from the kinetic theory of crystallization. This may simply be due to contaminants in the polymer which could have a weakly nucleating effect which is only significant when the homogeneous nucleation rates are low. An alternative possibility is that on the long timescales involved at these crystallization temperatures, segregation of PHB-rich areas which are able to nucleate may occur. However, the kinetic theory provides a reasonable model for the crystallization process over most of the temperature range studied.

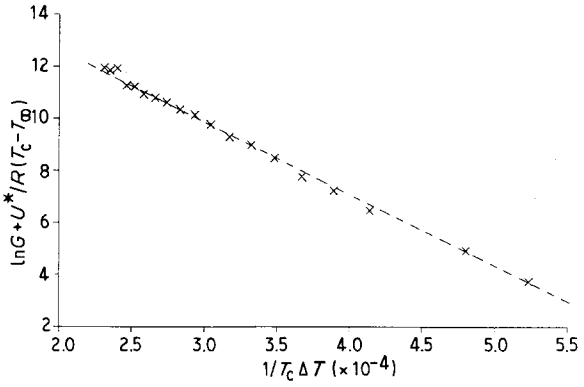

Figure 12 Analysis of growth rate data for PHB/7% HV.

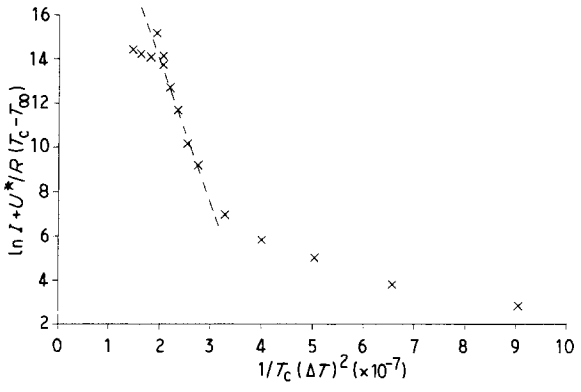

Figure 13 Analysis of nucleation rate data for PHB/7% HV.

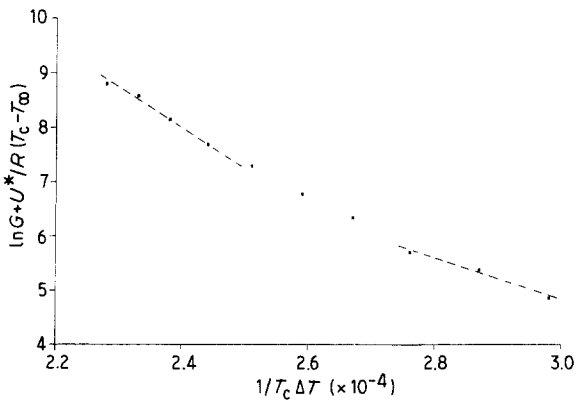

Figure 14 Analysis of growth rate data for PHB/23% HV.

Simple nucleation theory is unlikely to provide an adequate model for analysing the complex crystallization behaviour of the high copolymer PHB/23% HV. However, some further evidence for the segregation of HV from the crystal lattice at high crystallization temperatures is provided by the plot of $\ln G + U^*/R(T_c - T_\infty)$ against $1/T_c\Delta T$ shown in Fig. 14, where we have taken $T_m^0 = 186.2\,°C$ and all other values as for PHB. The results give a curve. If we simplistically consider a linear portion from the left-hand (high T_c) side of the graph, we obtain a gradient of $3.75 \times 10^{-9}\,J\,m^{-1}$ which is very close to the value obtained from PHB/7% HV. Alternatively, considering the right-hand (low T_c) side of the graph we get a gradient of $7.86 \times 10^{-9}\,J\,m^{-1}$. Taking an estimate from other work [16] for 23% HV copolymer of $\Delta H = 1.14 \times 10^8\,J\,m^{-3}$, this latter result yields a not unreasonable value of $\sigma\sigma_e = 11.63 \times 10^{-4}\,(J\,m^{-2})^2$. Thus the results are at least qualitatively consistent with the growth of high HV crystals at lower temperatures and low HV crystals at higher temperatures.

4. Discussion

First the results obtained on the PHB homopolymer will be discussed briefly and compared with our own previous studies [9]. In this work, as previously, the equilibrium melting points and, from growth and nucleation rate data, the surface free energies were determined.

The value of T_m^0 for PHB obtained in this work is $188 \pm 2\,°C$, while that obtained using the same method in our earlier study was $195 \pm 5\,°C$. In our previous study we used a second method, plotting the crystal melting point (T_m) against the inverse lamellar thickness ($1/l$) which yielded a higher value of $200 \pm 5\,°C$; we finally chose to use a value for T_m^0 of 197 °C, because it yielded a good linear plot for the growth rate data at low supercoolings.

It is noted that in the method of plotting T_m against $1/l$, the values of l used were those measured at room temperature and some thickening during heating is expected, as indicated by the double melting peaks shown in Fig. 3. Such changes in l during heating make this analysis unreliable. Thus it is preferable to use our more precise figure of $188 \pm 2\,°C$ obtained using the "Hoffman–Weeks" analysis. This change

in T_m leads directly to changes in the slopes of the $\log G$ against $1/T_c\Delta T$ and $\log I - 1/T_c(\Delta T)^2$ plots through the change in values of ΔT used; typically, for crystallization at $\sim 100\,^\circ C$, ΔT is 10% less in the present analysis. This change is largely responsible for the differences in the $\sigma\sigma_e$ and $\sigma^2\sigma_e$ values obtained in this, and our previous works. The values for σ and σ_e (8.2 and 94 erg cm^{-2}; 8.2×10^{-7} and 94×10^{-7} J cm^{-2}) obtained here are more plausible than those in our previous study of 30 and 38 erg cm^{-2} (30×10^{-7} and 38×10^{-7} J cm^{-2}). We should note that the analysis is based on the assumption that the nucleation of the PHB is homogeneous. We believe this to be justified because the nucleation rates we have observed are less than, but comparable with, those in our previous study [10] which obeyed homogeneous nucleation statistics.

Coming now to the 7% HV copolymer, we can see from the data in Figs 5, 12 and 13 that (with the exception of the high nucleation rates obtained at high temperatures discussed previously) this polymer is behaving in much the same way as the homopolymer, but with a reduced melting point (173 °C) and lower surface energies ($\sigma\sigma_e = 612$ (erg cm^{-2})^2; 612×10^{-7} (J cm^{-2})^2). Thus it seems reasonable to assume that the HV content of the crystals is more or less constant across the temperature range used in this work (20 to 100 °C), in which case the values of T_m^0 and $\sigma\sigma_e$ have real meaning. However, we must draw a note of caution; in another paper [16] we have shown, from density measurements, that there is a tendency for the crystals formed from PHB/HV copolymers to contain less HV when crystallized at higher temperatures. The effect is more pronounced at high HV contents, but is present even in a 7% copolymer. Accordingly, whilst the values of T_m^0, σ and σ_e obtained for this polymer may be of empirical utility in predicting nucleation and crystallization rates, they should be regarded as fitting parameters rather than thermodynamic quantities.

The effect of segregation of HV units into the non-crystalline phase becomes increasingly important for the higher HV copolymers and is reflected in the multiple melting peaks seen in the 23% HV polymer illustrated in Fig. 6. We have been able to identify five peaks. The peak at the highest temperature corresponds to a PHB-rich phase, or possibly to some pure PHB produced by the bacteria. Going down in temperature, the next three peaks correspond to the copolymer crystals formed at the crystallization temperature or to thickened crystals derived from them. The final low-temperature peak is due to material which was unable to crystallize at the elevated temperature, but which did crystallize on subsequent cooling. From the changes in sizes of the peaks, and from their positions, we can easily deduce that the number of HV units in the crystals formed at the crystallization temperature decreases markedly with increasing crystallization temperature, while the number of such crystals decreases.

5. Conclusions

We have shown that while PHB/HV copolymers appear quite similar to the PHB homopolymer in that all show a spherulitic texture, the rates of growth and nucleation are significantly reduced in the copolymers and we have confirmed our previous findings that there is considerable HV exclusion from the crystals, especially in high HV copolymers and at high crystallization temperatures.

References

1. M. LEMOIGNE, *Ann. Inst. Past.* **39** (1925) 144
2. J. MERRICK, *Photosynth. Bact.* **199** (1978) 219.
3. E. A. DAWES and P. J. SENIOR, *Adv. Microbiol.* **10** (1973) 138.
4. J. S. HERRON, J. D. KING and D. C. WHITE, *Appl. Environ. Microbiol.* **35** (1978) 251.
5. N. G. CARR, *Biochem. Biophys. Acta* **120** (1966) 308.
6. L. L. WALLEN and W. K. ROHWEDDER, *Environ. Sci. Technol.* **8** (1974) 576.
7. A. C. WARD, B. I. ROWLEY and E. A. DAWES, *J. Gen. Microbiol.* **102** (1977) 61.
8. P. A. HOLMES, in "Developments in Crystalline Polymers – 2", edited by D. C. Bassett (Elsevier, London, 1987) p. 1.
9. P. J. BARHAM, A. KELLER, E. L. OTUN and P. A. HOLMES, *J. Mater. Sci.* **19** (1984) 2781.
10. P. J. BARHAM, *ibid.* **19** (1984) 3826.
11. P. J. BARHAM and A. KELLER, *J. Polym. Sci. Polym. Phys. Edn* **24** (1986) 69.
12. S. J. ORGAN and P. J. BARHAM, *J. Mater. Sci. Lett.* **8** (1989) 621.
13. J. D. HOFFMAN and J. J. WEEKS, *J. Chem. Phys.* **37** (1962) 1723.
14. J. D. HOFFMAN, *Polymer* **24** (1983) 3.
15. F. P. PRICE, in "Nucleation", edited by A. C. Zettlemayer (Marcel Dekker, New York, 1969) p. 56.
16. P. A. BARKER, F. MASON and P. J. BARHAM, *J. Mater. Sci.* **25** (1990) p. 1952.

Received 15 March
and accepted 29 March 1990